Size dependence of charge order and magnetism in $Sm_{0.35}Ca_{0.65}MnO_3$

Cite as: AIP Advances **11**, 025313 (2021); https://doi.org/10.1063/9.0000122
Submitted: 22 October 2020 . Accepted: 18 January 2021 . Published Online: 08 February 2021

Lora Rita Goveas, K. S. Bhagyashree, K. N. Anuradha, and S. V. Bhat

Size dependence of charge order and magnetism in $Sm_{0.35}Ca_{0.65}MnO_3$

Cite as: AIP Advances 11, 025313 (2021); doi: 10.1063/9.0000122
Presented: 5 November 2020 • Submitted: 22 October 2020 •
Accepted: 18 January 2021 • Published Online: 8 February 2021

Lora Rita Goveas,[1,a)] K. S. Bhagyashree,[2] K. N. Anuradha,[3] and S. V. Bhat[2]

AFFILIATIONS

[1] Department of Physics, St. Joseph's College (Autonomous), Bangalore 560027, India
[2] Department of Physics, Indian Institute of Science, Bangalore 560012, India
[3] Department of Physics, Dr. Ambedkar Institute of Technology, Bangalore 560056, India

Note: This paper was presented at the 65th Annual Conference on Magnetism and Magnetic Materials.
[a)] **Author to whom correspondence should be addressed:** loragoveas@gmail.com

ABSTRACT

We report a systematic tracking of consequences of size decrease to nanoscale for charge order (CO) and magnetic properties of electron doped manganite $Sm_{0.35}Ca_{0.65}MnO_3$ by magnetization measurements. The bulk form of this system is charge ordered below 270 K and antiferromagnetic (AFM) below 130 K. The bulk sample and nanoparticles of various sizes (mean diameter ~ 15, 30, 90 nm) were synthesized by sol-gel technique. Our studies show that the robust CO in the bulk gets weakened by size reduction and the nanoparticles exhibit ferromagnetic (FM) ordering. Magnetization at high temperatures, in the paramagnetic region, reflecting the behaviour of the most part of the samples arising due to FM fluctuations caused by double exchange interaction is found to decrease as the particle size reduces. However, at low temperature the trend of FM magnetization as a function of the size is found to be reversed. This result is understood in terms of the dominance of surface effects where uncompensated bonds and an increase in the charge density at the surface layers lead to weak ferromagnetism which increases with decreasing size.

INTRODUCTION

Over the last few decades the doped perovskite manganites $RE_{1-x}A_xMnO_3$(RE, trivalent rare-earth ion; A, divalent alkaline earth ion) have fascinated scientific community due to the variety of phenomena like colossal magnetoresistance (CMR), charge order (CO), orbital order (OO) and phase separation(PS) exhibited by them.[1–6] The intimate mutual coupling of many degrees of freedom namely charge, spin, lattice and orbital in these strongly correlated systems produce huge responses to small perturbations. Currently the size induced effects in manganites like emergence of ferromagnetism (FM), suppression of CO, exchange bias (EB) effect, spin glass (SG) transition, magnetocaloric effect, training effect and memory effect have resulted in paving the way for many technological applications making the research in this field much exciting.[7–10]

CO in rare earth manganites is an interesting manifestation occurring due to interactions between phonons and charge carriers, resulting in localization of charge carriers at particular locations in the lattice below a certain characteristic temperature (T_{CO}). Predominance of Coulomb interactions over the kinetic energy of the charge carriers is the driving force of this phenomenon. The CO transition is indicated by an increase in resistivity, which is due to gradual freezing of the e_g electrons at the Mn^{3+} sites. A peak in magnetization is observed at T_{CO} occurring due to the FM fluctuations present for $T > T_{CO}$ making way for AFM fluctuations below T_{CO}. CO state is sensitive to perturbations like magnetic field,[11] pressure,[12] exposure to X-ray photons, structural and geometrical changes.[13] The suppression of CO and emergence of ferromagnetism consequent to the reduction of particle size was first reported by Rao *et al.*[14] Since then different groups have studied various systems and demonstrated that the CO phase could be suppressed by size reduction.[15–17]

Though the melting of CO and emergence of ferromagnetism has been the focus of a huge number of studies the mechanism responsible for such size effects are topic of intense debate. The phenomenological model proposed by Dong *et al.*, based on surface separation infers an increase in FM shell thickness with decrease

in grain size due to the relaxation of superexchange interaction on the surface layers.[18] Monte-Carlo simulation study on the CE-type CO/AFM phase has shown that an increase in the charge density at the surface layer due to unscreened Coulomb interactions results in suppressing the CO state leading to FM tendency.[19] 'Core-shell model' put forward by Zhang *et al.*,[20] explains that the anomalous behaviour of destruction of CO/AFM and emergence of FM is arising because of the uncompensated surface spins. However, Aliyu *et al.*,[21] find no evidence for a shell in their high resolution transmission electron microscopic study and conclude that excess of Mn^{3+} over Mn^{4+} in a single surface layer can cause the observed ferromagnetism. A recent theoretical study done using dynamical mean-field theory and density-functional theory showing that the structural changes caused by reduction in size is accountable for the size induced effects,[22] has been the subject of some controversy.[23]

It is well established that size reduction to nanoscale results in disappearance of charge ordered state and appearance of a FM phase at low temperature in half doped manganites.[15,24–26] Electron spin resonance (ESR) measurements on $Nd_{0.5}Ca_{0.5}MnO_3$ by Zhou *et al.*,[16] shows that though the magnetic measurements indicate the complete disappearance of CO in nanoparticles(size - 40nm), the temperature dependence of g-factor of ESR and linewidth clearly display the distinctive characteristic of the CO pointing towards the presence of short range charge order even though the long range charge order has disappeared.

The phase diagrams of doped manganites show that T_{CO} is maximum not for the composition x = 0.5, but around x = 0.6 the CO is found to be more robust.[27] When the size of RE and A ions in doped manganites become smaller as in the case of Sm and Ca, the $GdFeO_3$-type distortion becomes larger which favours the CO state to stabilize resulting in higher T_{CO}. The $Sm_{1-x}Ca_xMnO_3$ manganites have shown promising applications in the field of infrared emissivity, microwave absorption[28,29] and thermoelectric effect. In particular, $Sm_{0.35}Ca_{0.65}MnO_3$ (SCMO), the subject of the present investigation, has been found to have the highest emissivity contrast at 280 K corresponding to its T_{CO}.[30,31]

EXPERIMENTAL DETAILS

Sol-gel method was followed for the synthesis of samples. Stoichiometric amounts of high purity (≥99.9%) Sm_2O_3, $CaCO_3$ and $MnCO_3$ were first converted into nitrates and then subjected to hydrolysis and condensation followed by polymerisation. The precursor powder obtained was separated into numerous parts and each portion was annealed separately at temperatures 550 °C, 650 °C and 850 °C for about 6 hours. Heating the precursor at 1200 °C for 24 hours resulted in micrometer sized particles which we designate as bulk particles. Structural investigations were carried out by X-ray diffraction (XRD) using BRUKER D8 ADVANCE X-ray diffractometer with monochromatic radiation source Cu-Kα (λ = 1.54056 Å). The XRD patterns were analysed with Rietveld method using the software GSAS. Using transmission electron microscopy (TEM) and scanning electron microscopy (SEM) the particle sizes and morphology were found. The compositional examination was done by energy dispersive X-ray analysis (EDAX). Oxygen stoichiometry was measured by iodometric titration. Superconducting quantum interference device (SQUID) magnetometer at a field of 0.01 T was used to carry out magnetization measurements in the temperature range 10-300 K.

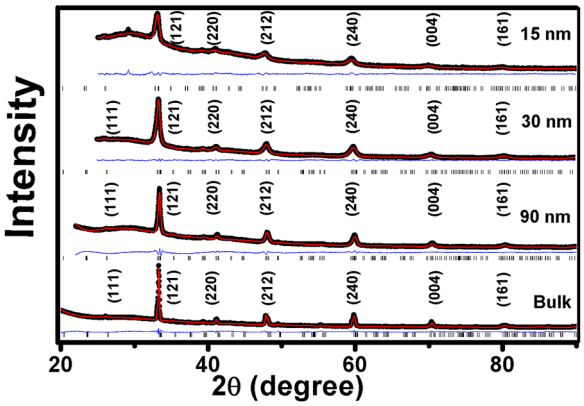

FIG. 1. Rietveld plots for various sizes indicated in the panel. The experimental data points are indicated by black solid dots, the calculated by red solid line and difference patterns by blue solid lines. The Bragg positions of the reflections are indicated by vertical lines below the patterns.

RESULTS AND DISCUSSION

The XRD patterns of all synthesised particles obtained at room temperature are given in Figure 1 which confirm single phase and crystalline nature with orthorhombic crystal structure. The decrease in the full width at half maximum (FWHM) of the diffraction peak with increase in annealing temperature indicates growth in particle size. Volume ($Å^3$) of unit cell calculated from the XRD profile fitting using the software GSAS are 222.78, 220.28, 219.76 and 219.23 respectively for 15nm, 30 nm, 90 nm and bulk particles. The shrinkage of volume due to size reduction is observed in $Pr_{0.5}Ca_{0.5}MnO_3$,[15,32] $La_{0.4}Ca_{0.6}MnO_3$,[17] $La_{0.9}Ca_{0.1}MnO_3$[33] whereas increase in cell volume with reduced size has been reported in $Nd_{0.5}Ca_{0.5}MnO_3$[24] and $Sm_{0.5}Ca_{0.5}MnO_3$.[34] The magnetic behaviour of the nano particles in all the above-mentioned systems are found to be similar though the structural changes observed are different.

The TEM images (not shown) of nanosamples reveal that the average particle size is about 15 nm, 30 nm and 90 nm for 550 °C, 650 °C and 850 °C sintered sample respectively. The samples are henceforth named as 15 nm, 30 nm, 90 nm and Bulk in the increasing order of their size. The SEM image (not shown) of Bulk showed that the grains are of a few micrometres in size. The cationic composition was confirmed using EDAX. The oxygen contents estimated by iodometric titration for bulk particles were determined to be 3.021 ± 0.015.

Temperature dependence of field cooled (FC) and zero field-cooled (ZFC) magnetizations (M) measured at H=100 Oe, between 10 K and 300 K for 15 nm, 30 nm, 90 nm and Bulk particles is shown in Figure 2. The bulk sample shows a clear CO peak at temperature 270 K and AFM transition at 130 K (Fig. 2 (b)) which is consistent with the observations reported earlier.[27] For the nanosamples, as the size of the particle reduces the CO transition peak is found to be of decreased intensity, broadened and shifted towards the lower temperature indicating that the CO phase is weakened in the nanosized

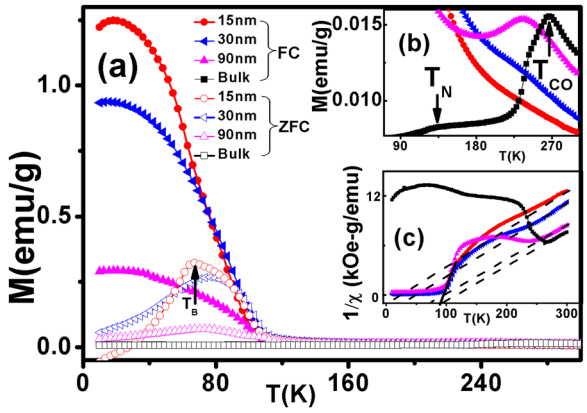

FIG. 2. (a) Temperature dependence of ZFC and FC magnetization at H = 100 Oe (solid fills for FC and hollow for ZFC). (b) FC curves at high temperature(c) Temperature variation of inverse dc susceptibility.

samples. For 15 nm the broad CO peak is found to have completely disappeared. While this could be an evidence for the absence of long-range charge order, short range CO can still be present and local probe techniques like electron paramagnetic resonance can help verify that possibility. The AFM transition peak is visibly absent in the case of all nanosamples. All the nanosamples show increase in magnetization with lowering temperature with a rapid rise below 100 K reflecting presence of FM behaviour at low temperatures. The FC and ZFC curves bifurcate around 100 K; ZFC exhibiting a peak shows a blocking temperature (T_B) which reduces with size of the particle. The irreversibility between FC and ZFC, the non-saturation of FC are an indication of strong anisotropy and glassy nature of spins in nanoparticle.[34]

The expanded view of the FC curves in the temperature range 300 - 90 K is shown as inset (b) to Figure 2. It is interesting to note from Figure 2(a) and (b) that closer to room temperature, as particle size decreases magnetization also decreases whereas at lower temperature as the particle size decreases magnetization increases. This reversal in the order of magnitude of magnetisation could be attributed to different behaviours of the spins on the surface and in the core of the particles. The magnetization at room temperature is due to FM fluctuations occurring in the paramagnetic region of the entire sample. As the temperature is reduced and the CO sets in, FM fluctuations of paramagnetic region begin to decrease giving way to AFM fluctuations resulting in a decrease in magnetization in the core. When the size of the particle decreases the core, size lessens eventually reducing the magnetization. But when the temperature is reduced further the magnetization in nanosamples increases due to the ordering of uncompensated spins at the surface of the nanoparticles. As particle size reduces surface effect rules over the core, consequently magnetization increases in the nanoparticles.[30] We provide more quantitative understanding of this behaviour next.

Figure 2(c) shows the plots of inverse susceptibility 1/χ vs temperature for the bulk as well as the three nanosized particle samples. It is seen that for each nano sample the plot contains two separate linear regions: the high temperature (HT) range, (~300 – 250 K) and the low temperature (LT) (~90 – 130 K). The two regions are

TABLE I. CW-parameters obtained by fitting CW-law for low temperature and high temperature regimes.

Sample	C_{HT} (emu-K/g-Oe)	o_{HT} (K)	C_{LT} (emu-K/g-Oe)	o_{LT} (K)
15 nm	0.0250 ± 0.0003	17 ± 4	0.0068 ± 0.0002	92 ± 7
30 nm	0.0243 ± 0.0004	31 ± 5	0.0060 ± 0.0002	95 ± 3
90 nm	0.0248 ± 0.0005	90 ± 5	0.0046 ± 0.0002	94 ± 7
Bulk	0.0247 ± 0.0005	111 ± 6		

separated by a transition region which is characterized by an initial upward change in 1/χ signalling development and dominance of AF correlations followed by a downward change indicating the development of FM correlations which eventually culminate in FM transitions. This behaviour is quite different from that of the bulk sample which has only the HT linear region and it does not undergo any FM transition. The data in the linear regions of all the samples are fitted to the Curie-Weiss law $\chi = C/(T - \Theta)$ (Fig. 2 (c)) and the Curie constant $C (= (N_A/3k_B)\mu^2_{eff}$ where N_A is the Avogadro number, k_B is the Boltzmann constant and μ_{eff} is the effective magnetic moment per ion) and the paramagnetic Curie temperature Θ (which is a measure of the strength of the inter-spin coupling,[35] in the present case, strength of the ferromagnetic exchange interactions) are extracted and are presented in Table I. The fitting errors are also indicated for each value of C_{HT}, C_{LT}, Θ_{HT} and Θ_{LT}.

The following points are to be noted: (a) Θ_{HT} decreases with decreasing particle size implying that in the high temperature region the Zener double exchange mediated FM correlations weaken as the size is reduced. (b) In contrast, Θ_{LT} is independent of the nanoparticle size. This implies that the strength of the FM correlations in the surface layer is independent of the nano particle size in as much as it is believed that the origin of the ferromagnetism in nanoparticles is in the uncompensated spins on the surface shell of the nanoparticles.[19] This interesting result, being reported for the first time to the best of our knowledge, requires further experimental and theoretical confirmation and understanding. (c) C_{HT} and C_{LT} also exhibit contrasting behaviour in that whereas C_{HT} is seen to be independent of particle size, C_{LT} increases with decreasing size. The latter behaviour could be understood as a consequence of the fact that as the size decreases, the relative contribution of the surface shell to the measured magnetization increases.

The field dependent magnetization studies done at different temperatures for bulk and nanoparticles are shown in Figures 3(a) at 50 K and Figures 3(b) at 280 K. The bulk shows a linear variation at both the temperatures, confirming the absence of a ferromagnetic phase. The formation of ferromagnetism at low temperature is evident from the hysteresis loop at 50 K in the field dependent magnetization of the nanosamples (15 nm and 30 nm). Magnetization does not saturate even up to 5 T magnetic fields for all the nanoparticles showing the presence of residual AFM in the particles. In our system the fraction of Mn^{3+} and Mn^{4+} ions is 0.35: 0.65 and if all the spins were to be ferromagnetically aligned, the value of μ_{eff} would be $6.321\mu_B$ per ion. The spontaneous magnetization M_S obtained by the linear extrapolation of the high field magnetization above 2.5 T to H = 0 is found to be 6.5817 emu/g ($\mu_{eff} = 0.2141\ \mu_B$ per ion ~ 3.4% of the ideal value) and 7.997 emu/g ($\mu_{eff} = 0.2603\ \mu_B$ per ion ~ 4.1% of the ideal value) for 30 nm and 15 nm respectively. This

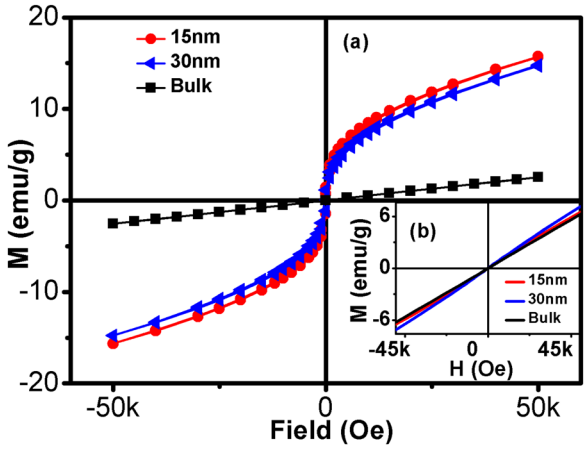

FIG. 3. Field dependence of magnetization of (a) at T = 50 K and (b) T = 150 K.

indicates that only a very small fraction of the sample is ferromagnetic, consistent with the understanding of the presence of only surface ferromagnetism in the nanoparticles.

CONCLUSION

Nanoparticles of average diameter 15 nm, 30 nm, and 90 nm were synthesized by adopting sol-gel technique and their properties were compared with bulk samples. Structural analysis shows that there is an increase in unit cell volume with decrease in particle size. The magnetization curve of bulk shows a clear CO peak at temperature 270 K and AFM transition at 130 K. Magnetization studies of the nanosamples, indicate that as the size of the particle reduces the CO transition peak is found to be broadened and shifted towards the lower temperature indicating that the CO phase is weakened in the nanosized samples. As the particle size is reduced to 15 nm, the broad CO peak is found to have completely disappeared indicating that long range CO is no longer present though, at this stage the presence of short-range charge ordering cannot be ruled out. Our studies are consistent with the suppression of the CO and the appearance of the weak ferromagnetism in the nanoparticles arising from the dominance of the surface effects.

ACKNOWLEDGMENTS

K.N.A. acknowledges Technical Education Quality Improvement. Programme III (Grant No. TEQIP III), NPIU/SPIU and Dr. Ambedkar Institute of Technology, Bangalore, India for financial support. S.V.B. thanks The National Academy of Sciences, India for financial support.

DATA AVAILABILITY

The data that support the findings as well as the TEM and SEM micrographs of this study are available from the corresponding author upon reasonable request.

REFERENCES

[1] J. M. D. Coey, M. Viret, and S. von Molnár, Adv. Phys. **48**, 167 (1999).
[2] T. Hotta, A. L. Malvezzi, and E. Dagotto, Phys. Rev. B **62**, 9432 (2000).
[3] A. Arulraj, P. N. Santhosh, R. S. Gopalan, A. Guha, A. K. Raychaudhuri, N. Kumar, and C. N. R. Rao, J. Phys. Condens. Matter **10**, 8497 (1998).
[4] L. Gorkov and V. Kresin, Phys. Rep. **400**, 149 (2004).
[5] Y. Tokura, Rep. Prog. Phys. **69**, 797 (2006).
[6] S. S. Rao and S. V. Bhat, J. Phys. Condens. Matter **21**, 196005 (2009).
[7] T. Zhang, G. Li, T. Qian, J. F. Qu, X. Q. Xiang, and X. G. Li, J. Appl. Phys. **100**, 094324 (2006).
[8] A. Sawa, T. Fujii, M. Kawasaki, and Y. Tokura, Appl. Phys. Lett. **88**, 232112 (2006).
[9] M. Aparnadevi and R. Mahendiran, J. Appl. Phys. **113**, 013911 (2013).
[10] S. N. Jammalamadaka, S. S. Rao, S. V. Bhat, J. Vanacken, and V. V. Moshchalkov, AIP Adv **2**, 012169 (2012).
[11] A. Guha, A. Ghosh, A. K. Raychaudhuri, S. Parashar, A. R. Raju, and C. N. R. Rao, Appl. Phys. Lett. **75**, 3381 (1999).
[12] R. Mahendiran, M. R. Ibarra, A. Maignan, F. Millange, A. Arulraj, R. Mahesh, B. Raveau, and C. N. R. Rao, Phys. Rev. Lett. **82**, 2191 (1999).
[13] M. R. Lees, J. Barratt, G. Balakrishnan, D. M. Paul, and C. Ritter, Phys. Rev. B **58**, 8694 (1998).
[14] S. S. Rao, K. N. Anuradha, S. Sarangi, and S. V. Bhat, Appl. Phys. Lett. **87**, 182503 (2005).
[15] T. Zhang and M. Dressel, Phys. Rev. B **80**, 014435 (2009).
[16] S. Zhou, Y. Guo, J. Zhao, L. He, C. Wang, and L. Shi, J. Phys. Chem. C **115**, 11500 (2011).
[17] E. Rozenberg, M. Auslender, A. Shames, D. Mogilyansky, I. Felner, E. Sominskii, A. Gedanken, and Y. Mukovskii, Phys. Rev. B **78**, 052405 (2008).
[18] S. Dong, F. Gao, Z. Q. Wang, J.-M. Liu, and Z. F. Ren, Appl. Phys. Lett. **90**, 082508 (2007).
[19] S. Dong, R. Yu, S. Yunoki, J.-M. Liu, and E. Dagotto, Phys. Rev. B **78**, 064414 (2008).
[20] T. Zhang, T. Zhou, T. Qian, and X. Li, Phys. Rev. B **76**, 174415 (2007).
[21] H. D. Aliyu, J. M. Alonso, P. de la Presa, W. E. Pottker, B. Ita, M. Garcia-Hernández, and A. Hernando, Chem. Mater. **30**, 7138 (2018).
[22] H. Das, G. Sangiovanni, A. Valli, K. Held, and T. Saha-Dasgupta, Phys. Rev. Lett. **107**, 197202 (2011).
[23] V. Markovich and G. Jung, Phys. Rev. Lett. **108**, 129701 (2012).
[24] S. S. Rao, S. Tripathi, D. Pandey, and S. V. Bhat, Phys. Rev. B **74**, 144416 (2006).
[25] S. Zhou, Y. Guo, C. Wang, L. He, J. Zhao, and L. Shi, Dalton Trans **41**, 7109 (2012).
[26] S. K. Giri and T. K. Nath, Int. J. Nanosci. **10**, 285 (2011).
[27] C. Martin, A. Maignan, M. Hervieu, C. Autret, B. Raveau, and D. Khomskii, Phys. Rev. B **63**, 174402 (2001).
[28] L. Chen, C. Lu, Z. Fang, Y. Lu, Y. Ni, and Z. Xu, Mater. Lett. **93**, 308 (2013).
[29] L. Chen, C. Lu, Y. Zhao, Y. Ni, J. Song, and Z. Xu, J. Alloys Compd. **509**, 8756 (2011).
[30] M. Hervieu, A. Barnabé, C. Martin, A. Maignan, F. Damay, and B. Raveau, Eur. Phys. J. B-Condens. Matter Complex Syst. **8**, 31 (1999).
[31] P. Laffez, C. Napierala, M. Zaghrioui, V. Ta Phuoc, A. Hassini, and M. R. Ammar, Appl. Phys. Lett. **93**, 151910 (2008).
[32] T. Sarkar, P. K. Mukhopadhyay, A. K. Raychaudhuri, and S. Banerjee, J. Appl. Phys. **101**, 124307 (2007).
[33] E. Rozenberg, A. Shames, M. Auslender, G. Jung, I. Felner, J. Sinha, S. Banerjee, D. Mogilyansky, E. Sominski, A. Gedanken, Y. Mukovskii, and G. Gorodetsky, Phys. Rev. B **76**, 214429 (2007).
[34] S. K. Giri, A. Poddar, and T. K. Nath, AIP Adv **1**, 032110 (2011).
[35] A. Czachor, J. Magn. Magn. Mater. **139**, 355 (1995).